ARTICLE OPEN ACCESS

New recessive mutations in *SYT2* causing severe presynaptic congenital myasthenic syndromes

Stéphanie Bauché, PhD, Alain Sureau, PhD, Damien Sternberg, MD, John Rendu, PharmD, PhD, Céline Buon, Julien Messéant, PhD, Myriam Boëx, PhD, Denis Furling, PhD, Julien Fauré, PhD, Xénia Latypova, MD, PhD, Antoinette Bernabe Gelot, MD, PhD, Michèle Mayer, MD, Pierre Mary, MD, Sandra Whalen, MD, Emmanuel Fournier, MD, PhD, Isabelle Cloix, MD, Ganaelle Remerand, MD, Fanny Laffargue, MD, Marie-Christine Nougues, MD, Bertrand Fontaine, MD, PhD, Bruno Eymard, MD, PhD, Arnaud Isapof, MD, and Laure Strochlic, PhD

Correspondence
Dr. Bauché
stephanie.godard-bauche@upmc.fr

Neurol Genet 2020;6:e534. doi:10.1212/NXG.0000000000000534

Abstract

Objective

To report the identification of 2 new homozygous recessive mutations in the synaptotagmin 2 (*SYT2*) gene as the genetic cause of severe and early presynaptic forms of congenital myasthenic syndromes (CMSs).

Methods

Next-generation sequencing identified new homozygous intronic and frameshift mutations in the *SYT2* gene as a likely cause of presynaptic CMS. We describe the clinical and electromyographic patient phenotypes, perform ex vivo splicing analyses to characterize the effect of the intronic mutation on exon splicing, and analyze the functional impact of this variation at the neuromuscular junction (NMJ).

Results

The 2 infants presented a similar clinical phenotype evoking first a congenital myopathy characterized by muscle weakness and hypotonia. Next-generation sequencing allowed to the identification of 1 homozygous intronic mutation c.465+1G>A in patient 1 and another homozygous frameshift mutation c.328_331dup in patient 2, located respectively in the 5′ splice donor site of *SYT2* intron 4 and in exon 3. Functional studies of the intronic mutation validated the abolition of the splice donor site of exon 4 leading to its skipping. In-frame skipping of exon 4 that encodes part of the C2A calcium-binding domain of SYT2 is associated with a loss-of-function effect resulting in a decrease of neurotransmitter release and severe pre- and postsynaptic NMJ defects.

Conclusions

This study identifies new homozygous recessive *SYT2* mutations as the underlying cause of severe and early presynaptic form of CMS expanding the genetic spectrum of recessive *SYT2*-related CMS associated with defects in neurotransmitter release.

From the Sorbonne Université, INSERM, UMRS974, Centre de Recherche en Myologie, Hôpital de la Pitié-Salpêtrière, Paris, (S.B., A.S., C. B., J.M., M.B., D.F., E. F., B.F., B.E., A.I., L.S.); CHU APHP (D.S., J.R., J.F., X.L., A.B.G., M.M., P.M., S.W., E.F., I.C., G.R., F.L., M.C.N., B.F., B.E., A.I.); Aix-Marseille University, INSERM, INMED, Campus de Luminy, Marseille, France (A.B.G.); UFR Cardiogénétique et Myogénétique, Hôpital de la Pitié-Salpêtrière, APHP, Paris (D.S.); UF de génétique clinique, CRMR Anomalies du développement et syndromes malformatifs, APHP, Hôpital Armand Trousseau, Paris, France (S.W.); Université de Grenoble Alpes, INSERM, CHU Grenoble Alpes, GIN (J.R., J.F., X.L.); CHU Clermont Ferrand (I.C., G.R., F.L.); and Reference Centre for Neuromuscular Pathologies "Nord/Est/Ile-de France" Paris (A.B.G., M.M., P.M., S.W., M.C.N., B.F., B.E., A.I.).

Funding information and disclosures are provided at the end of the article. Full disclosure form information provided by the authors is available with the full text of this article at Neurology.org/NG.

The Article Processing Charge was funded by the authors.

Glossary

AChR = acetylcholine receptor; **CMS** = congenital myasthenic syndrome; **ENMG** = electroneuromyography; **NGS** = next-generation sequencing; **NIV** = noninvasive ventilation; **NMJ** = neuromuscular junction; **PBS** = phosphate-buffered saline; **RNS** = repetitive nerve stimulation; **SYT2** = synaptotagmin 2.

Congenital myasthenic syndromes (CMSs) are rare genetic diseases due to malfunction of neuromuscular transmission caused by mutations in genes critical for proper neuromuscular junction (NMJ) development and function and characterized by a fatigable muscle weakness.[1]

Among more than 30 disease-causing genes, mutations in those encoding presynaptic proteins have been identified as responsible for increasingly complex phenotypes of CMS.[2–4] Synaptotagmin 2 (*SYT2*) is a synaptic vesicle protein essential for neurotransmitter release, mostly expressed at the NMJ, acting as a calcium sensor mediated by 2 tandem C2 domains (C2A and C2B).[5,6] Previously, dominant mutations in the SYT2 C2B domain have been linked to a presynaptic CMS and/or motor neuropathies.[7–9] However, recently, a homozygous recessive mutation in the SYT2 C2B domain causing presynaptic CMS has been reported, raising the question of the frequency of this rare recessive form.[10]

Here, we report 2 new intronic and frameshift homozygous recessive mutations in the SYT2 C2A domain causing early and severe presynaptic forms of CMS. The clinical description of the 2 patients from 2 distinct consanguineous families first evoked a congenital myopathy evolving toward CMS forms. We demonstrate that the intronic mutation causes in-frame skipping of *SYT2* exon 4 that leads to a loss-of-function effect associated with altered NMJs maintenance and synaptic transmission, whereas the frameshift mutation introduces a premature stop codon abolishing SYT2 protein synthesis. Our study emphasizes the link between SYT2 and presynaptic forms of hereditary recessive CMS, which appears to be as frequent as those related to dominant mutations in *SYT2*.

Methods

Standard protocol approvals, registrations, and patient consents

Samples were collected according to national and European regulations (Article L1243-3 and L1243-4), and participants gave informed consents approved by national ethic committees (DC-2012-1535 and AC-2012-1536).

Patient evaluation

Children were referred to the Center of Reference for Neuromuscular Diseases for Diagnostic. Evaluations including electrophysiologic studies were performed on Viasys machine (Viasys Healthcare) using standardized protocols. Electroneuromyography (ENMG) including repetitive nerve stimulation (RNS) at 3 Hz and nerve conduction studies have been performed on 4 nerve/muscles for patient 1. The percentage of decrement was calculated between the first and fourth responses. A sample of patient 1's quadriceps muscle was taken and compared with deltoid muscle from individuals without any neuromuscular disorder (control).

DNA analysis and sequencing

Patients' genomic DNA was isolated from blood samples using the Qiasymphony diagnostic sample preparation DNA Midi Kit on a Qiasymphony nucleic acid extraction machine (Qiagen) or on a Maxwell nucleic acid extraction machine (Promega). The identification of variants was performed on the basis of 2 different panels of genes including CMS-causing genes. The patient and his relatives' genomic DNA were amplified by PCR and Sanger-sequenced using Primer3 software for primer design. Reference transcript used for the *SYT2* gene was NM_177402.4.

For patient 1, next-generation sequencing (NGS)-based screening of 41 genes was performed using a SeqCap EZ capture design (NimbleGen) and a MiSeq sequencer (Illumina). Variants were identified through a bioinformatics pipeline (GenoDiag, Paris, France) and filtered according to their frequency in the general population and in patient's samples.

For patient 2, NGS-based screening of 133 genes was performed using SureSelect XT2 capture design (Agilent) and sequenced on a NextSeq (Illumina). Annotation was realized using VarAFT software.[11]

The primers used both for PCR and sequencing were *SYT2*-Ex4F: 5′-TCGGTCCTCCCCTTTTAACT-3′; *SYT2*-Ex4R: 5′-GCTGTTTCTATCCCCCTTCC-3′ for patient 1 and *SYT2*-Ex3F: 5′-AAATCACTCATGGGTGTGTGG-3′; *SYT2*-Ex3R: 5′-TTGTTCTCCTTCACTGTCTTTCC-3′ for patient 2.

Ex vivo splicing assay

To evaluate the impact of the intronic mutation identified in patient 1 on splicing, an ex vivo splicing assay using patient genomic DNA was performed.

Cloning *SYT2* exon 4 mutation in the splicing reporter minigene PCAS2

The PCAS2 plasmid allows insertion of exonic DNA sequences into natural intron 3 of *SERPING1/CINH* gene as previously described.[12,13] *SYT2* exon 4 was amplified from control and patient 1 genomic DNA using 2X platinum Taq (Thermo Fisher Scientific) and primers *SYT2* intron 3 F:

AGTCGGATCCCTAGGGGTTCTGATGGGCC and *SYT2* intron 4 R: GACTACGCGTAAGCCAGCATCAATGTCCA. PCR conditions were 98°C for 30 seconds, followed by 30 cycles with 98°C for 10 seconds, 60°C for 15 seconds, 72°C for 30 seconds, and 72°C for 5 minutes. After PCR product separation and purification (NucleoSpin Gel and PCR Clean-up, Macherey Nagel), there are digested with BamHI and MluI (New England Biolabs) and inserted into pCAS2 vector. After selected colonies (α-select silver, Bioline), plasmid DNA was purified (NucleoSpin Plasmid, Mini kit for plasmid DNA, Macherey Nagel) and controlled by sequencing (Eurofins Scientific, France).

Cell culture and transient transfection

HEK293T cells were cultured in Dulbecco Modified Eagle Medium with 4.5 g of glucose (Thermo Fisher Scientific, France) supplemented with 10% fetal bovine serum (Thermo Fisher Scientific, France) and 100 U/mL penicillin/streptomycin (Thermo Fisher Scientific, France) at 37°C in a humidified 5% CO_2 atmosphere. Four micrograms per well of WT or mutant construct DNA was transiently transfected in 6-well plates (TPP plate; Sigma-Aldrich) using FuGENE6 (Promega).

RT-PCR

After 24 hours of transfection, total RNA was purified and reverse transcribed (QuantiTect SYBR Green RT-PCR Kit, Qiagen), and the resulting complementary DNA was amplified by PCR with primer minigen exon 2 F: GCTGACGTCGCCGCCCATCAC and minigen exon 3 R: CCCAGTAGTGGGCTGGGTAGG and Dream Taq Green (Thermo Fisher Scientific). Cycle conditions were 94°C for 3 minutes, followed by 30 cycles with 94°C for 10 seconds, 57°C for 20 seconds, 72°C for 50 seconds, and 72°C for 5 minutes. After separation by electrophoresis, RT-PCR products were visualized in ultraviolet light (GENI Gel Documentation System, Syngene). PCR products were purified with NucleoSpin Gel (Macherey Nagel) and sequenced by Eurofins to validate the splicing patterns.

Patient muscle biopsy analysis

To evaluate the direct or indirect pathogenic effect of intronic mutation at the synaptic level, a neuromuscular morphological analysis was performed for patient 1. The muscle biopsy of patient 2 has not been performed due to his very young age.

NMJ analysis

The NMJ-rich zone was determined by revealing cholinesterase activity using the classical Koelle method.[14] After 1 hour fixation with 4% paraformaldehyde in 1X-phosphate-buffered saline (PBS), muscle samples were saturated with 0.1 M glycine in PBS overnight at 4°C, blocked with 3% bovine serum albumin in PBS for 30 minutes, and incubated with primary antibodies overnight at 4°C. Alexa 488–conjugated anti-mouse or anti-rabbit IgG secondary antibodies (1:300, Thermo Fisher scientific) were used for immunofluorescence detection at room temperature for 4 hours after PBS washes. To visualize postsynaptic acetylcholine receptors (AChRs), we used tetramethylrhodamine -labeled α-bungarotoxin (1:1,000, α-BGT, Molecular Probes; Life Technologies). For terminal axon, terminal Schwann cells, and immunofluorescence staining of SYT1 and SYT2, the following primary antibodies were used: monoclonal anti-neurofilament 165 kDa (1:500, 2H3 clone, Developmental Studies Hybridoma Bank, IA), monoclonal anti-neurofilament 200-kDa antibodies (1:500, RT97 clone, Boehringer Ingelheim, Germany), polyclonal anti-S100 antibody (1:100, Dako/Agilent), rabbit anti-SYT1 antibody (1:100, Abcam, Cambridge, UK), and a rabbit anti-SYT2 antibody (1:100, Thermo Fisher Scientific), respectively. Whole mount specimens were observed using the laser scanning microscope (LSM) 510 confocal laser-scanning microscope equipped with a 63x objective (LSM 510, Carl Zeiss, Inc) after mounted in Vectashield (H-1000, Vector Laboratories).

Muscle morphology

To analyze the muscle fiber morphology, fiber type distribution, and accumulations, transversal cryosections of 10 μm were stained, respectively, with conventional hematoxylin-eosin, modified Gomori trichrome, nicotinamide adenine dinucleotide hydride tetrazolium reductase, and succinate dehydrogenase.

Data analysis and statistics

Statistical analysis and histogram were performed using GraphPad StatMate software (Prism8). In all figures, the data are presented as mean ± SEM. The statistical results were presented as follows: ns = no significant ($p > 0.05$), $^{*}p < 0.05$, $^{**}p < 0.005$, $^{***}p < 0.001$, and $^{****}p < 0.0001$. The NMJ morphometric analyses were performed using a new standardized ImageJ-based platform workflow NMJ-morph adapted for humans to facilitate comparative normal and pathologic analysis of pre- and postsynaptic components such as overall NMJ area and degree of AChR fragmentation, the most critical parameters for defining synaptic morphology in vivo as previously described.[15] SYT1 and SYT2 quantification of staining intensity was performed by measuring the average fluorescence intensity of specific antibodies against SYT1 or SYT2 using ImageJ software (version 2.0.0).

Data availability

Materials, methods, and data essentials to conduct this project are described in detail in the Methods section.

Results

Clinical presentation

The 2 affected patients were born from 2 distinct consanguineous families (figure 1A). Table 1 summarizes the clinical characteristics of both patients.

Patient 1 presented severe and global hypotonia, muscle weakness, hypomimic face, flat chest, poor crying, and feeding since birth. Although the patient's clinical course was stable, a

Figure 1 Genetic and electrophysiologic features of recessive *SYT2* mutations

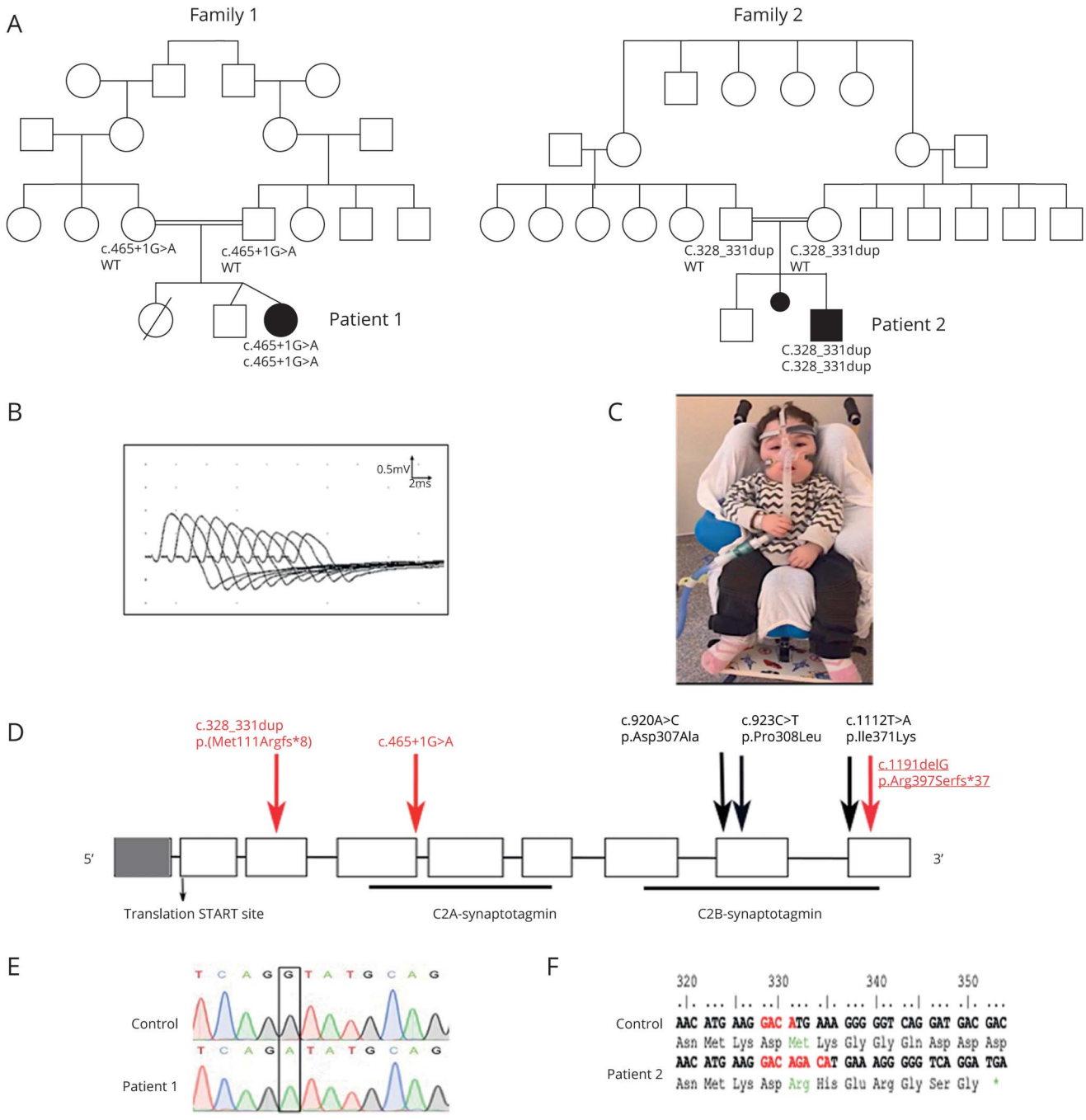

(A) The family 1 and 2 pedigrees revealed that only patients 1 and 2 (in black) are affected in the families and support the recessive autosomal heredity from consanguineous families at second degree with grandparents who are sister and brother in both cases. (B) Decrement at RNS (3 Hz) was observed from 25% to 39% in 3 muscles/nerve. (C) Image of patient 2 showing a severe congenital hypotonia with muscle weakness preventing him from holding his head, respiratory failure requiring NIV, and a constant feeding tube. (D) Position of the identified mutations on the structure of SYT2 protein. Intronic and frameshift mutations identified in this study are indicated in red, respectively, in the C2A domain and in exon 3, whereas the homozygote recessive mutation described in the literature is noted in underlined red. The dominant missense mutations described in the C2B domain of SYT2 are represented in black. Exons encoding C2A and C2B domains are underlined. The codon START is indicated at the beginning of exon 2; exon 1 does not encode for any amino acids. (E) Sanger sequencing revealed a 465+1G>A substitution in patient 1 cDNA compared with the control. Red: the 4 nucleotides of the control (GACA), which are duplicated in patient 2. Green: modified amino acids. (F) Sequence alignment of the SYT2 region corresponding to nucleotides 319 to 354 (amino acids 107–118) of patient 2 compared with the control. Red: the 4 nucleotides of the control (GACA), which are duplicated in patient 2. Green: modified amino acids. *Premature stop codon. NIV = noninvasive ventilation.

slight fluctuating ptosis was present. She had delay of motor milestone and developed scoliosis without tendon reflexes. Motor and sensory nerve conduction revealed very low compound muscle action potential responses and normal sensory responses (table 2). Moreover, a decrement at (RNS, 3 Hz) was observed from 25 to 39% in 3 muscles (figure 1B).

Table 1 Clinical features of patients affected by recessive SYT2 mutations

	Patient 1	Patient 2
Characteristic at diagnosis		
Pregnancy	Twin pregnancy, uneventful	Uneventful
Birth	Term delivery	Term delivery
Age, mo	48	8
Sex	Female, birth	Male, birth
Mutations	c.465+1G>A	c.328_331dup; p.(Met111Argfs*8)
First symptoms (age)	At birth	At birth
Clinical description	Major hypotonia, hypomimic face	Major hypotonia, hypomimic face
	Global muscle weakness, poor feeding	Global muscle weakness
	No swallowing difficulties, flat chest	Respiratory insufficiency
	Poor crying	Lack of succion refexe and swallowing
Fluctuations	Mild ptosis	No
Exacerbation, myasthenic crisis	No, no	Yes: apneic crisis
Supportive care	No	Enteral nutrition by tube
	—	Assisted breathing (NIV) 24 h/24
Course characteristics		
Response to therapy	+++, combined effect of AChEI with salbutamol and 3,4-DAP	+++, combined effect of AChEI with salbutamol and 3,4-DAP
Symptoms during course	Hypomimic face, hypotonia, muscle weakness, and fluctuating ptosis	Hypotonia, muscle weakness, respiratory insufficiency, sucking difficulties
Motor function evolution	Good improvement of motor skills, tonus, and strength	Moderate improvement of motor skills, tonus, and strength
Fluctuations	No	No
Exacerbation, myasthenic crisis	No, no	No, apneic crisis
Orthopedic retraction	Secondary knee flessum	Secondary knee flessum
Scoliosis	Yes	No
Respiratory function	Normal	Reduce NIV to sleep
Swallowing	Normal	No
Motor milestones	Head control at 16 mo	No head control at 11 mo, global hypotonia
	Sitting position with support at 2.5 y	—
Neurologic explorations		
ENMG (age)	8 mo	ND
Decrement 3 Hz	39% (spinal nerve)	ND
Increment 10 Hz	Could not be tested	ND
Myopathic pattern	Yes (proximal muscles)	ND
Muscle biopsy	Minor remodeling with a predominance of type I fibers and atrophy of type II fibers	ND
Brain MRI	Normal	Normal
ABR	ND	Normal
EEG	ND	Normal

Abbreviations: ABR = audiometry brainstem response; AChEI = acetylcholinesterase inhibitor; ENMG = electroneuromyography; ND = not done; NIV = noninvasive ventilation; 3,4-DAP = diaminopyridine; +++ = good improvement.

Table 2 Patient 1 motor nerve conduction studies

Nerve	CMAP recording site	CMAP amplitude (mV)	MNCV (m/s)	% Change following
Peroneal nerve R.	Peroneal	0.4	37	—
	Fibular	0.4	—	—
Tibial nerve L.	Under malleolar	0.3	47	—
	Popliteal fossa	0.1	—	—
Median R.	Wrist	0.8	—	−25
	Elbow	0.3	35	—
Spinal R.	Trapezius	1.1	—	−39
Spinal L.	Trapezius	0.8	—	−35

Nerve	SNAP recording site	SNAP amplitude (mV)	MNCV (m/s)
Median R.	Wrist	24	56
	Elbow	7	—
Cubital R.	Wrist	22	—
	Elbow	3.5	—

Abbreviations: CMAP = compound muscle action potential; MNCV = motor nerve conduction velocity; SNAP = sensory nerve action potential.

In addition, needle EMG showed a myopathic pattern in proximal muscles without denervation (data not shown). Single-fiber EMG was not performed. Muscle biopsy analysis revealed a minor muscle remodeling with a predominance of type I fibers and atrophy of type II fibers in agreement with a CMS muscle profile (data not shown). The therapeutic association of AChEI (pyridostigmine), 3,4-diaminopyridine (DAP) (FIRDAPSE), and salbutamol from 8 months was well tolerated and led to regular and significant improvement of the child's motor skills. Withdrawal of therapy for electrophysiologic tests led to worsening of symptoms with reappearance of major hypotonia and generalized muscle weakness. She was born from a twin pregnancy unremarkable, and a previous child died 2 days after birth with anoxic-ischemic encephalopathy, likely related to CMS.

Patient 2 presented severe congenital hypotonia and muscle weakness, with respiratory insufficiency and poor feeding from birth. Since birth, he presented multiple anoxic episodes with desaturation and bradycardia despite noninvasive ventilation (NIV). He had increasing swallowing difficulties since age 2 months and from then required feeding tube (figure 1C). Electrophysiologic testing and muscle biopsy could not be performed. Treatment with pyridostigmine, FIRDAPSE, and salbutamol started at age 7 months, allowed the stabilization of the clinical course without anoxic episodes. An improvement of his motor skills with spontaneous movements of the upper and lower limbs, as well as a reduction of the NIV to sleep was possible at age 11 months without improvement in head control or swallowing.

In both cases, the clinical presentations first evoked a severe congenital myopathy that then progressed toward muscle fatigue and delay of motor milestones with no deformity of the feet, including pes cavus or hammer toes. Acetylcholine receptor, MuSK, or voltage-gated calcium channel antibodies were negative in both patients. The serum level of creatine kinase was normal. Parents of both children are asymptomatic, and ENMG performed in parents of patient 1 did not reveal any anomaly.

Genetic diagnosis

After NGS sequencing and variant filtering, 2 pathogenic homozygous variations in the *SYT2* gene (NM_177402.4) and a short list of nonpathogenic predicted consequence variants were obtained (table 3).

For patient 1, the intronic *SYT2* variation c.465+1G>A affects the canonical splice donor site of exon 4, resulting in a loss of the splice donor site of exon 4 and to an in-frame skipping of exon 4 encoding a part of the SYT2 C2A domain (figure 1, D and E).

For patient 2, the frameshift variation c.328_331dup (p.Met111Argfs*8), localized in exon 3 of *SYT2*, is due to the duplication of 4 nucleotides (GACA) causing a shift in the reading frame that introduce a premature stop codon after translation of 8 new amino acids (figure 1, D and F). Thus, an abnormally short polypeptide and nonsense-mediated decay of the resulting messenger RNA that would result in the absence of SYT2 protein synthesis were predicted. Sanger sequencing confirmed the homozygous *SYT2* variations in both patients and their heterozygous state in each asymptomatic parent.

Table 3 Variants retained after sequencing and filtering in patients

Patient 1				
Gene name	***CACNA1S***	***CHAT***	***RYR1***	***SYT2***
Locus number	NM_000069.2	NM_020549.4	NM_000540.2	NM_177402.4
HGVS nucleotide	c.4077C>A	C.2222G>A	c.2682G>A	c.465+1G>4
HGVS protein	p.Tyr1359*	p.Arg741Lys	p.Pro894Pro	—
Gene consequences	Stop gain	Missense	Synonymous, splice region	Splice donor, intron
Coverage	467	449	328	366
Alternate read count	228	237	161	363
Proportion of reads	49%	53%	49%	99%
Allelic transmission	Heterozygous	Heterozygous	Heterozygous	Homozygous
Inheritance	Maternal	Maternal	Paternal	Paternal and maternal
Patient 2				
Gene name		***PREPL***	***RYR1***	***SYT2***
Locus number		NM_001171606	NM_000540.2	NM_177402.4
HGVS nucleotide		c.1517A>G	C.5000G>A	c.328_331dup
HGVS protein		p.Tyr506Cys	p.Arg1667His	p.(Met111Argfs*8)
Gene consequences		Missense	Missense	Frameshift
Coverage		787	776	415
Alternate read count		378	372	415
Proportion of reads		48%	48%	100%
Allelic transmission		Heterozygous	Heterozygous	Homozygous
Inheritance		Maternal	Maternal	Paternal and maternal

Abbreviations: *CACNA1S* = calcium voltage-gated channel subunit alpha1 A; *CHAT* = choline acetyltransferase; HGVS = Human Genome Variation Society; *PREPL* = prolyl endopeptidase like; *RYR1* = ryanodine receptor 1.

Mutation in intron 4 of SYT2 leads to exon 4 skipping

To evaluate the impact of the intronic mutation in *SYT2* intron 4 at the molecular level, we generated a PCAS2 minigene construct including control or patient genomic DNA sequences spanning *SYT2* exon 4 (figure 2A, a and b). RT-PCR analysis of the minigene transcripts revealed, as predicted, that the c.465+1G>A mutation induced a complete skipping of exon 4 (figure 2B). RT-PCR products sequencing confirmed exon 4 skipping triggered by the mutation. These results indicate that the *SYT2* intronic variation abolishes the splice donor site of exon 4 leading to a 120 bp truncation (40 amino acids) in the N-terminal part of the SYT2 C2A domain.

NMJ abnormalities on patient 1 with mutation in *SYT2* intron 4

The pathogenic impact of *SYT2* exon 4 skipping at the synaptic level on the patient's muscle biopsy shows a major disruption of pre- and postsynaptic architectures (figure 3A). Immunostaining of motor axon appeared drastically disturbed with more than 80% of remodeled NMJ corresponding to partially innervated NMJ with thin and unbranched terminal axon contacting dispersed and fragmented synaptic gutters (figure 3, A and B). The remaining 20% of NMJs analyzed appeared fully denervated, without terminal axon, and neoformed NMJ with thin unbranched terminal axon contacting small cups of concentrated AChR clusters (figure 3, A and B). Moreover, a postsynaptic deficit corresponding to a significant decrease in the AChR area without affecting the number of AChR fragments per NMJ in the patient compared with the control is observed (figure 3B). Therefore, the categorization of the synaptic profiles supports that a large proportion of NMJs is remodeled or denervated in the patient compared with the control (figure 3B).

Although SYT2 is the major isoform at the NMJ, SYT1 is also expressed but to a lesser extent. Thus, to determine whether truncation of the C2A domain affects both synaptotagmin expressions at the NMJ, we evaluated the levels of SYT1 or SYT2 expression at the NMJ in the patient's muscle biopsy

Figure 2 Patient 1 exon 4 skipping using the splicing reporter minigene PCAS2

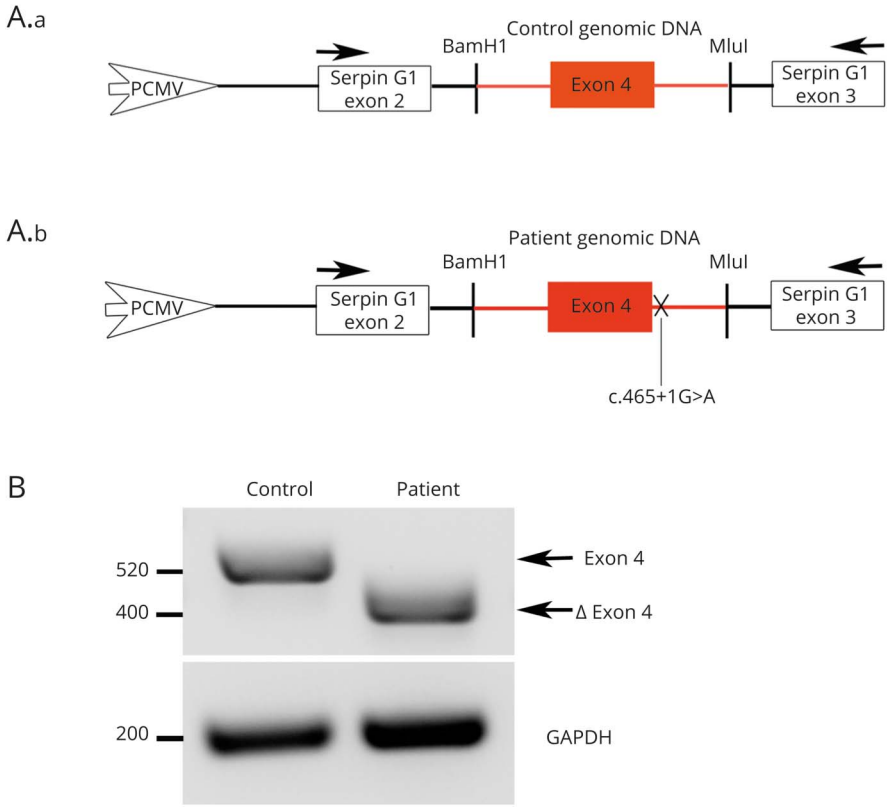

(A) Schematic representation of the pCAS2-SYT2-exon4. Genomic DNA of the patient and the control has been inserted into natural intron 3 of SERPING1/CINH gene surrounded by exons 2 and 3. Arrows: primers used for RT-PCR analysis. (B) After transfection in HEK293T cells and RT-PCR analysis of the minigene transcripts containing control or patient genomic DNA, agarose gel electrophoresis shows that the c.465+1G>A mutation induces the loss of 120 nucleotides corresponding to the complete patient's exon 4 skipping. Resulting PCR products are labeled exon 4 for the control (520 bp) and Δ exon 4 for the patient (400 bp). GAPDH, amplified to confirm equal amounts of starting cDNA, shows comparable transcripts quantity between the patient and the control.

compared with control (20 NMJs for each conditions) (figure 4A). For all NMJs analyzed, the quantification of the fluorescence intensity level showed a two-fold reduction of SYT2 expression and a significant increase of 40% of SYT1 immunostaining compared with the control (figure 4B). Of interest, the percentage of positive NMJs for SYT1 or SYT2 staining showed that although SYT2 is expressed in all NMJs in the control, only 20% of endplates displayed SYT2 immunostaining in the patient. Concomitantly, when SYT2 expression is reduced in the patient, we observed a moderate increase of 10% endplates expressing SYT1 compared with control (figure 4B). These results demonstrate that exon 4 skipping leads to reduced level of SYT2 immunostaining at the human NMJ associated with the upregulation of SYT1 expression.

Discussion

In this study, we describe in 2 consanguineous families 2 new homozygous recessive mutations in the *SYT2* gene responsible for severe and early presynaptic forms of CMS. In both patients, congenital myopathy was primary evoked with major neonatal hypotonia associated with global muscle weakness without foot deformities that differs from previous clinical presentation described in SYT2 dominant forms.[7–9] These clinical features were reinforced by the myopathic aspect of the muscle observed in both muscular histopathologic and electromyographic studies of patient 1. In the 2 cases, CMS diagnosis was demonstrated by major arguments including a significant decrement for patient 1 and a positive response to the same therapeutic association of AChEI, salbutamol, and 3,4-DAP resulting in a significant motor skills improvement.

Our study is in line with the recent identification of a new recessive homozygous mutation (c.1191delG; p.Arg397-Serfs*37) in the SYT2 C2B domain coding region as the underlying cause of severe presynaptic CMS associated with atrophy and denervation in a consanguineous patient.[10] The clinical presentation, very similar to ours, showed an early onset of severe hypotonia, global weakness, areflexia with moderate bulbar deficit, and fatigable ptosis worsening during the day,[10] which differs from those described in the 3 dominant *SYT2* cases with lower limb distal involvement with foot deformities mimicking Charcot-Marie-Tooth neuropathy.[7–9] Moreover, electrophysiologic studies have shown an reduction of compound muscle action potential amplitude at rest with an initial 1,000% facilitation, followed by a progressive decline at RNS (30–50 Hz) different from those observed in Lambert-Eaton myasthenic syndrome cases as well as a denervation with a highly polyphasic motor unit and potential duration identical to those observed in the recessive

Figure 3 Morphologic analysis of NMJ in patient 1

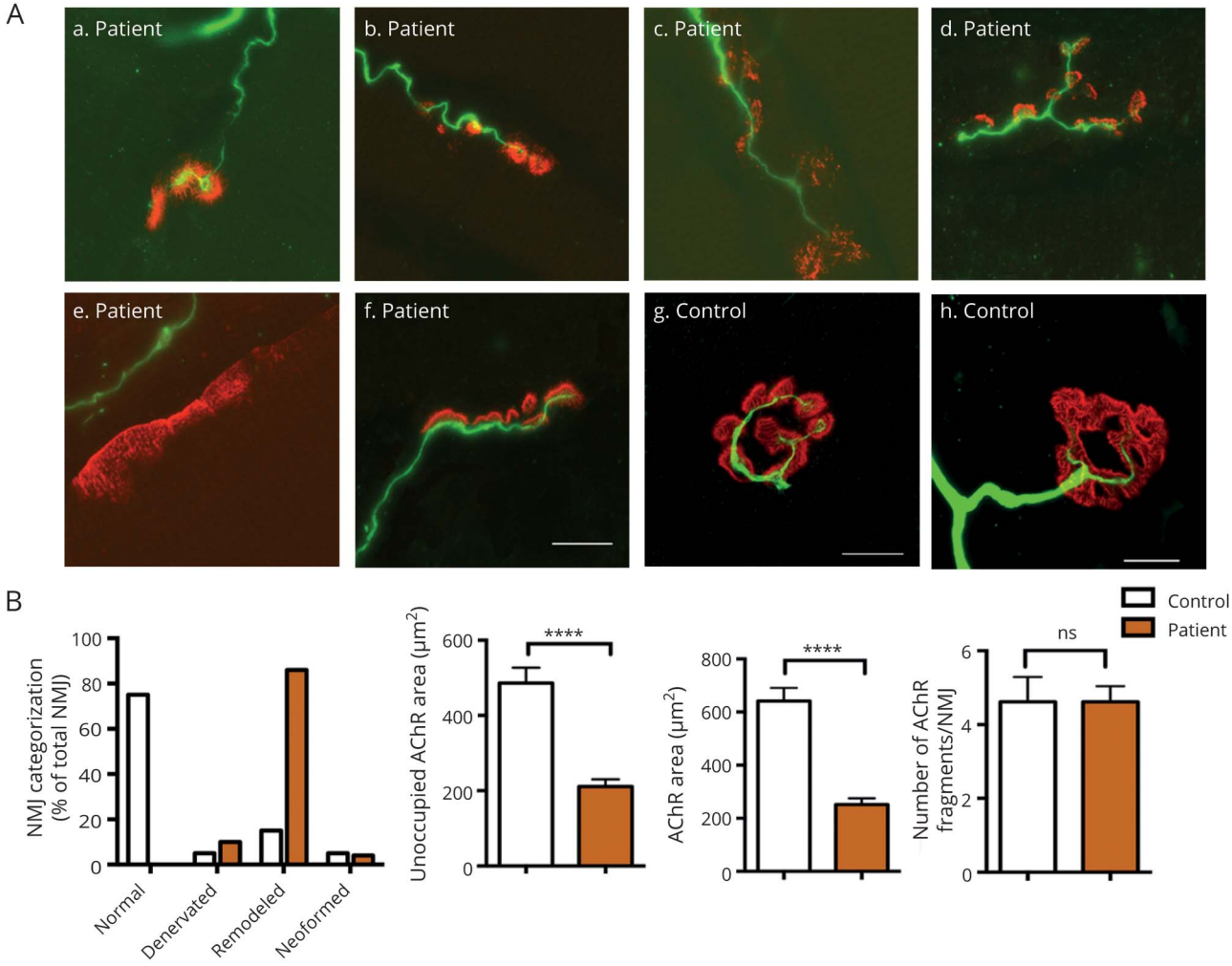

(A) Representative NMJ confocal pictures of the patient muscle biopsy immunostained with an anti-neurofilament antibody in green to label the motor axons and with α-bungarotoxin in red for postsynaptic AChR. Representative control, neoformed, remodeled, and denervated NMJ pictures are shown. Scale bar: 10 µm. (B) Histogram of NMJs classification into 4 categories and postsynaptic morphometric analyses. Changes in NMJs distribution with a majority of remodeled NMJs were observed in the patient compared with the control. Using human-adapted NMJ-morph workflow analysis on confocal z-stack projections of individual NMJs, histograms of postsynaptic components such as AChR fragment number, AChR area, or unoccupied AChR area showed a major remodeling of NMJs in the patient compared with the control. The same parameters were applied to the patient and the control. ****$p < 0.0001$. All error bars are SEM. AChR = acetylcholine receptor; NMJ = neuromuscular junction; ns = no significant change ($p > 0.05$).

and dominant *SYT2* forms.[7–10] In our study, due to the young age of the patients, without excluding his presence, no high-frequency stimulation or exercise contraction allowing the observation of an incremental response could be demonstrated. Moreover, needle EMG of a myopathic pattern associated with a denervation process at the NMJ of patient 1 was revealed, whereas only a denervation profile was reported in the recessive or dominant *SYT2* mutations.[7–10] Of note, in contrast to findings reported by the Maselli group showing an improvement in muscle fatigue with the combination of 3,4-DAP and pyridostigmine, without efficacy of albuterol, the additional combination of salbutamol in our patients resulted in a significant improvement in their still persistent fatigue.[10] Indeed, although the molecular mechanism of salbutamol remains unclear, it is widely used in CMS and ameliorates the adverse effect of long-term pyridostigmine on NMJ structure.[16]

SYT2 is an essential protein responsible for synchronous vesicle release at the NMJ which C2B domain is critical for driving synaptic fusion,[5,17] while the C2A domain plays a crucial role in fast synchronous neurotransmitter release,[18,19] each of the two domains is involved in calcium binding in different ways.[20,21] Previous studies indicate that the loss of normal calcium binding by heterozygote missense mutations in SYT2 C2B domain reduces neurotransmitter release leading to an autosomal dominant presynaptic CMS associated with a gain-of-function effect, which partly explains the incremental response.[7–9,22] In contrast, our data showed that the loss-of-

Figure 4 Expression level of SYT-1 and -2 in patient 1

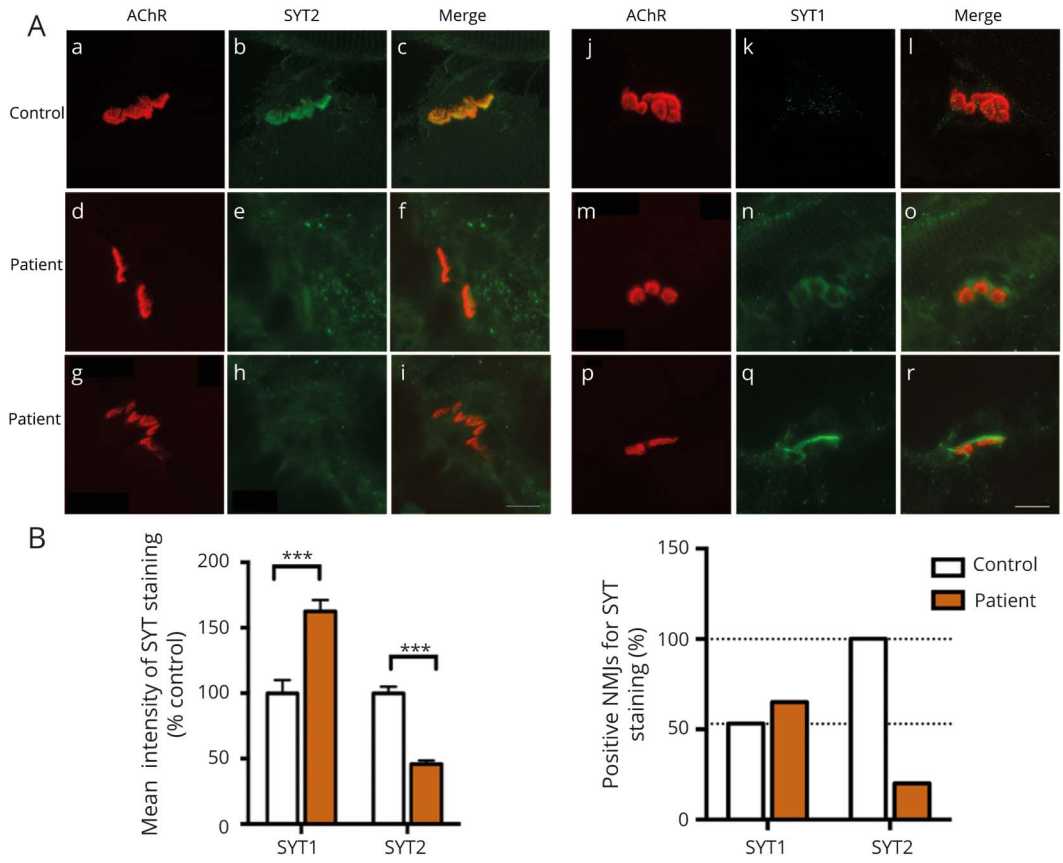

(A) Immunostaining study of SYT1 and SYT2 in green together with AChR in red to visualize the synaptic area. All NMJs express SYT2 in the control (a–c), whereas SYT2 staining intensity is decreased in the patient's NMJs (d–i). A large majority of NMJs expressing a low immunostaining intensity of SYT1 were detected in the control (j–l) while an increase in staining intensity and number of NMJs expressing SYT1 was observed in patient's samples (m–r). Scale bar: 10 µm. (B) Histograms of mean intensity and percentage of positive NMJs for SYT1 and SYT2 staining on confocal z-stack projections of all patient's NMJs analyzed, including negative immunostaining, compared with the control. Number of NMJs analyzed: 50 for the patient and 30 for the control. ***$p < 0.0001$. All error bars are SEM. AChR = acetylcholine receptor; NMJ = neuromuscular junction; SYT = synaptotagmin.

function effect resulting from homozygous loss of SYT2 expression induces a strong reduction in evoked release of neurotransmitter.[23] Of interest, heterozygous dominant mutations described so far (substitutions in the C2B domain) result in a dominant negative effect directly affecting the calcium binding, whereas the reported homozygous recessive mutations cause either premature stop codon or exon skipping of the C2A domain, leading to a loss-of-function effect of SYT2 compensated by overexpression of SYT1, as demonstrated in this study.[7–9,22] These studies show that dominant mutations do not affect calcium binding in the same way as recessive mutations, which may partly explain the electrophysiologic and phenotypic differences observed in the patients. Thus, the nonlethal compensatory mechanism of synaptic transmission in the SYT2 KO mouse, likely due to expression of a second calcium sensor for fast release allowing to compensate the loss of SYT2, may explain the early and severe presynaptic phenotypes observed in our study.[23]

NMJ morphometric analysis from patient 1 muscle biopsy showed strong pre- and postsynaptic abnormalities corresponding to an increased denervation-reinnervation process. This is in line with a study demonstrating the importance of the SYT2 C2A domain in the neurite outgrowth and may explain the presynaptic abnormalities observed in patient 1's NMJs.[24] Furthermore, probably due to presynaptic alterations and neurotransmission defects, postsynaptic abnormalities with a significant decrease in the synaptic area without loss of AChR fragments have also been observed.

Although mice deleted from the *SYT2* gene die around 3 weeks of general weakness, they do not show any developmental phenotype as do homozygous SYT2-I377N mutant mice in which decreased expression of SYT2 associated with increased expression of SYT1 is observed in the spinal cord.[23,25] Although the reason for the coexpression of several synaptotagmins detecting calcium at the synaptic level remains unclear, it seems likely that the evolutionary diversification of SYT1 into oligomeric complexes plays a regulatory role at a synaptic level when SYT2 is decreased.[23] These results are consistent with the overexpression of SYT1 when SYT2 is decreased in patient

1, and it can be hypothesized that is also the case in patient 2 in the complete absence of SYT2. Of note, studies of dominant negative *SYT1* mutations in humans have reported clinical features of motor defects in early childhood without neurotransmission analysis.[26] This raises the matter of neuromuscular impairment in young patients with a recessive heterozygous mutation in the *SYT1* gene.

In conclusion, we report the identification, of 2 novel homozygous recessive mutations in *SYT2* in 2 consanguineous families responsible for a severe and early presynaptic CMS. This report describes recessive loss-of-function mutations in *SYT2*, one of which corresponds to the C2A domain and completes previous data on dominant SYT2-CMS associated with gain-of-function effect and the homozygous recessive mutation in the SYT2 C2B domain involved in presynaptic CMS form. Overall, our results allow us to consider that homozygous recessive mutations in both SYT2 C2A and C2B domains are associated with SYT2 loss-of-function effect, partly compensated by the overexpression of SYT1 leading to NMJ defects and resulting in similar complex forms of presynaptic CMS that may be as frequent as dominant mutations described so far.[7–9] Thus, this study may be useful for the diagnosis and treatment for patients with presynaptic CMS due to recessive *SYT2* mutations and highlights the need for early diagnosis of CMS as a treatable condition in massive hypotonia in neonates. Besides, this study underlines the interest of a massive sequencing of updated and differential gene panels for the genetic diagnosis of CMS,[27] allowing the revelation of new mutations, new mode of transmission, new molecular pathomechanisms, and new genotype-phenotype correlations for known genes such as for the *SYT2* gene.

Acknowledgment

The authors thank the family members for their contribution in this study. They also thank Dr. Sophie Nicole for giving them the PCAS2 Minigene obtained by Material Transfer Agreement (MTA) with INSERM UMRS1079 Laboratory.

Study funding

Supported by AFM-Téléthon and Fondation de l'avenir grant number AP-RM-18-022.

Disclosure

The authors report no disclosures relevant to the manuscript. Full disclosure form information provided by the authors is available with the full text of this article at Neurology.org/NG.

Publication history

Received by *Neurology: Genetics* June 18, 2020. Accepted in final form September 25, 2020.

Appendix Authors

Name	Location	Contribution
Stéphanie Bauché, PhD	Institute of Myology, Paris	Study design and conceptualization, analyzed the data, and drafted the manuscript for intellectual content
Alain Sureau, PhD	Institute of Myology, Paris	Major role in ex vivo splicing assay and revised the manuscript
Damien Sternberg, MD	APHP, Paris	Major role in genetic data and identification of SYT 2 mutation in patient 1
John Rendu, PharmD, PhD	Université de Grenoble, Grenoble	Major role in genetic data and identification of SYT 2 mutation in patient 2
Céline Buon	Institute of Myology, Paris	Role in genetic and histology data
Julien Messéant, PhD	Institute of Myology, Paris	Revised the manuscript and technical assistance for NMJ-morph workflow
Myriam Boëx, PhD	Institute of Myology, Paris	Revised the manuscript
Denis Furling, PhD	Institute of Myology, Paris	Revised the manuscript
Julien Fauré, PhD	Université de Grenoble, Grenoble	Role in genetic data
Xénia Latypova, MD, PhD	Université de Grenoble, Grenoble	Role in genetic data
Antoinette Bernabe Gelot, MD, PhD	Trousseau Hospital, Paris	Major role in histology study
Michele Mayer, MD	Trousseau Hospital, Paris	Role in clinical data
Pierre Mary, MD	Trousseau Hospital, Paris	Realized the human muscle biopsy
Sandra Whalen, MD	Trousseau Hospital, Paris	Major role in genetic data for patient 1
Emmanuel Fournier, MD, PhD	Institute of Myology, Paris	Major role in electrophysiologic data and revised the manuscript
Isabelle Cloix, MD	Clermont Ferrand Hospital, Clermont Ferrand	Major role in clinical data
Ganaelle Remerand, MD	Clermont Ferrand Hospital, Clermont Ferrand	Major role in clinical data
Fanny Laffargue, MD	Clermont Ferrand Hospital, Clermont Ferrand	Major role in clinical data
Marie-Christine Nougues, MD	Trousseau Hospital, Paris	Major role in clinical data and revised the manuscript

Continued

Appendix *(continued)*

Name	Location	Contribution
Bertrand Fontaine, MD, PhD	Institute of Myology, Paris	Revised the manuscript
Bruno Eymard, MD, PhD	Institute of Myology, Paris	Major role in clinical data and revised the manuscript
Arnaud Isapof, MD	Trousseau Hospital, Paris	Major role in clinical data and revised the manuscript
Laure Strochlic, PhD	Institute of Myology, Paris	Critical revision of the manuscript for intellectual content

References

1. Tintignac LA, Brenner HR, Rüegg MA. Mechanisms regulating neuromuscular junction development and function and causes of muscle wasting. Physiol Rev 2015; 95:809–852.
2. Rodríguez Cruz PM, Palace J, Beeson D. The neuromuscular junction and wide heterogeneity of congenital myasthenic syndromes. Int J Mol Sci 2018;19:1677.
3. Nicole S, Azuma Y, Bauché S, Eymard B, Lochmüller H, Slater C. Congenital myasthenic syndromes or inherited disorders of neuromuscular transmission: recent discoveries and open questions. J Neuromuscul Dis 2017;4:269–284.
4. Engel AG. Congenital myasthenic syndromes in 2018. Curr Neurol Neurosci Rep 2018;18:46.
5. Lee J, Guan Z, Akbergenova Y, Littleton JT. Genetic analysis of synaptotagmin C2 domain specificity in regulating spontaneous and evoked neurotransmitter release. J Neurosci 2013;33:187–200.
6. Rickman C, Archer DA, Meunier FA, et al. Synaptotagmin interaction with the syntaxin/SNAP-25 dimer is mediated by an evolutionarily conserved motif and is sensitive to inositol hexakisphosphate. J Biol Chem 2004;279:12574–12579.
7. Herrmann DN, Horvath R, Sowden JE, et al. Synaptotagmin 2 mutations cause an autosomal-dominant form of lambert-eaton myasthenic syndrome and nonprogressive motor neuropathy. Am J Hum Genet 2014;95:332–339.
8. Whittaker RG, Herrmann DN, Bansagi B, et al. Electrophysiologic features of SYT2 mutations causing a treatable neuromuscular syndrome. Neurology 2015;85:1964–1971.
9. Montes-Chinea NI, Guan Z, Coutts M, et al. Identification of a new SYT2 variant validates an unusual distal motor neuropathy phenotype. Neurol Genet 2018;4:e282.
10. Maselli RA, Linden HVD, Ferns M. Recessive congenital myasthenic syndrome caused by a homozygous mutation in SYT2 altering a highly conserved C-terminal amino acid sequence. Am J Med Genet A 2020;10:1002.
11. Desvignes JP, Bartoli M, Delague V, et al. VarAFT: a variant annotation and filtration system for human next generation sequencing data. Nucleic Acids Res 2018;46:W545–W553.
12. Gaildrat P, Killian A, Martins A, Tournier I, Frébourg T, Tosi M. Use of splicing reporter minigene assay to evaluate the effect on splicing of unclassified genetic variants. Methods Mol Biol 2010;653:249–257.
13. Tournier I, Vezain M, Martins A, et al. A large fraction of unclassified variants of the mismatch repair genes MLH1 and MSH2 is associated with splicing defects. Hum Mutat 2008;29:1412–1424.
14. Couteaux R, Taxi J. Distribution of the cholinesterase activity at the level of the myoneural synapse. Comptes Rendus Hebd Seances Acad Sci 1952;235:434–436.
15. Jones RA, Reich CD, Dissanayake KN, et al. NMJ-morph reveals principal components of synaptic morphology influencing structure-function relationships at the neuromuscular junction. Open Biol 2016;6:160240.
16. Vanhaesebrouck AE, Beeson D. The congenital myasthenic syndromes: expanding genetic and phenotypic spectrums and refining treatment strategies. Curr Opin Neurol 2019;32:696–703.
17. Mackler JM, Drummond JA, Loewen CA, Robinson IM, Reist NE. The C(2)B Ca(2+)-binding motif of synaptotagmin is required for synaptic transmission in vivo. Nature 2002;418:340–344.
18. Stevens CF, Sullivan JM. The synaptotagmin C2A domain is part of the calcium sensor controlling fast synaptic transmission. Neuron 2003;39:299–308.
19. Wen H, Linhoff MW, McGinley MJ, et al. Distinct roles for two synaptotagmin isoforms in synchronous and asynchronous transmitter release at zebrafish neuromuscular junction. Proc Natl Acad Sci 2010;107:13906–13911.
20. Young SM, Neher E. Synaptotagmin has an essential function in synaptic vesicle positioning for synchronous release in addition to its role as a calcium sensor. Neuron 2009;63:482–496.
21. Guan Z, Bykhovskaia M, Jorquera RA, Sutton RB, Akbergenova Y, Littleton JT. A synaptotagmin suppressor screen indicates SNARE binding controls the timing and Ca2+ cooperativity of vesicle fusion. eLife 2017;6:e28409.
22. Shields MC, Bowers MR, Fulcer MM, et al. Drosophila studies support a role for a presynaptic synaptotagmin mutation in a human congenital myasthenic syndrome. PLoS One 2017;12:e0184817.
23. Pang ZP, Melicoff E, Padgett D, et al. Synaptotagmin-2 is essential for survival and contributes to Ca2+ triggering of neurotransmitter release in central and neuromuscular synapses. J Neurosci 2006;26:13493–13504.
24. Kabayama H, Takei K, Fukuda M, Ibata K, Mikoshiba K. Functional involvement of synaptotagmin I/II C2A domain in neurite outgrowth of chick dorsal root ganglion neuron. Neuroscience 1999;88:999–1003.
25. Pang ZP, Sun J, Rizo J, Maximov A, Südhof TC. Genetic analysis of synaptotagmin 2 in spontaneous and Ca2+-triggered neurotransmitter release. EMBO J 2006;25: 2039–2050.
26. Baker K, Gordon SL, Grozeva D, et al. Identification of a human synaptotagmin-1 mutation that perturbs synaptic vesicle cycling. J Clin Invest 2015;125:1670–1678.
27. Krahn M, Biancalana V, Cerino M, et al. A National French consensus on gene lists for the diagnosis of myopathies using next-generation sequencing. Eur J Hum Genet 2019;27:349–352.